Journal of Thermal Analysis and Calorimetry, Vol. 89 (2007) 1, 101–107

METASTABLE EFFECTS ON MARTENSITIC TRANSFORMATION IN SMA Part II. The grain growth effects in Cu–Al–Be alloy

A. Sepulveda[1], *R. Muñoz*[1], *F. C. Lovey*[2], *C. Auguet*[3], *A. Isalgue*[3] *and V. Torra*[3*]

[1]FCFM-DIMEC, Universidad de Chile, Beauchef 850, Santiago, Chile
[2]Centro Atómico and Instituto Balseiro, 8400 S.C. de Bariloche, Argentina
[3]CIRG, DFA, ETSECCPB, UPC, Campus Nord B4, 08034 Barcelona, Catalonia, Spain

The efficiency of shape memory alloy (SMA) as damper and/or standard actuator is truly enhanced when the material can be cycled without any relevant accumulation of the permanent deformation (i.e. under 0.5% for several hundreds of cycles). The particular properties of the CuAlBe alloy permit relevant grain growth with reasonable reduction of mechanical properties (from 300–350 to 250–300 MPa at fracture). Samples prepared with an appropriate heat thermal treatment (HTT) and relevant mean diameter of grain avoids accumulative deformation for series of cycles (near 500) up to 3.5% of deformation. The analysis of different wires of CuAlBe alloy shows, in the first part of HTT, a proportionality between the grain surface and the time at 1123 K. In the last part of the HTT the grain growth shows an increased complexity related with interactions between the grain boundaries and the external surface of the samples.

Keywords: *aging, creep, CuAlBe, Cu-based alloys, grain growth, martensitic transformation, SMA*

Introduction

The publication in 1993 of one issue of the Bulletin of the Materials Research Society centered on Smart Materials can be considered the start point for the explosive growth of their applications. In fact, shape memory alloys (SMA) and other types of smart materials and systems (i.e., piezo-electrics, magnetostrictive, magneto-rheologic fluids and so on) are being progressively introduced in lectures of engineering courses. Also, in the last years, the SMA have being the object of various new industrial applications [1–5]. In single crystal or in polycrystalline samples the Cu–Al–Be is one of the main acknowledged alloys as, for instance, Nitinol (or NiTi) [6, 7] and other Cu and Fe based alloys. See, for instance, [6, 8] for a general overview of SMA.

SMA present, under the appropriate experimental conditions, two different behaviors: the shape memory effect and, at increased temperature, the superelastic one, both related to the martensitic transformation: a first order phenomena, with hysteresis. The transformation can be used in damping via the internal conversion of mechanical into thermal energy. Thus, the particular characteristics of that transformation between metastable phases induce changes (classical and not-classical) in the material properties. For instance, the transformation temperature is related to composition and thermal treatments. Also, external and internal heat contributions (such as latent heat and frictional ones) modify the position of the hysteresis cycle in the stress-strain space, via the Clausius–Clapeyron equation. In fact, the non-classical contributions related to diffusion processes also require an evaluation: changes in atomic order slowly modify the equilibrium temperature between the phases. The link between atomic order and transformation temperature is a well-acknowledged effect in metals and alloys [9, 10]. In SMA these are slow processes, but each time-scale associated with a specific application in an alloy requires an explicit consideration [11–13]. In the standard thermomechanical applications the coexistence effects and the actions induced by external thermodynamic forces in the parent phase [14] are generally not considered.

Damping is one of the relevant problems in civil structures [15, 16]. Because of their damping capacities, SMA have been proposed as materials for energy dissipative devices to be used in mechanical and civil engineering applications [17–19]. The position of the hysteretic stress-strain cycle is temperature dependent. A representation, in σ, ε, T coordinates, is outlined in Fig. 1. At temperatures close to the Ms the hysteresis width induces that, at zero load, the material remains partially transformed. See, for instance, the point a (cycle c_1) in Fig. 1. To ensure that a damper runs correctly it is necessary that stress (σ) satisfy $0 \le \sigma \le \sigma_{pd}$ and the strain (ε) satisfy $0 \le \varepsilon \le \varepsilon_{\pi}$. If the stress (or strain) were too high, classical plastic deformation in the martensitic phase would occur. For damping purposes, the hysteresis stress width ($\Delta\sigma_h$) has to be taken into account. Note that, for example, in most civil engineering application,

* Author for correspondence: vtorra@fa.upc.edu

1388–6150/$20.00

Akadémiai Kiadó, Budapest, Hungary
Springer, Dordrecht, The Netherlands

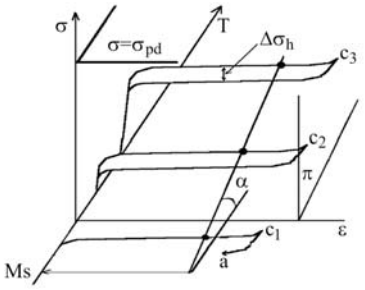

Fig. 1 Outline of the hysteretic behavior in a SMA represented in σ, ε, *T* coordinates. The slope α determines the Clausius–Clapeyron equation (dσ/d*T* in coexistence zone). $\Delta\sigma_h$ mean hysteresis width. Ms is the martensite start temperature. The π plane establishes the maximal deformation without accumulative and permanent deformation. c_1, c_2 and c_3 are three stress-strain cycles at progressively increased temperatures

the summer–winter temperature changes would displace the hysteretic cycles via the Clausius–Clapeyron coefficient (see the α slope changing the level of cycles c_2 and c_3 in Fig. 1), thus the self-heating and all thermal effects induced by atomic contributions need to be appropriately considered and, only when are not relevant for the application, neglected. In other words, only when the material in their working state always remains inside the thermoelastic window, plastic deformation is fully avoided (Fig. 1). An advantage of the superelastic effect (see superelastic c_2 and c_3 cycles in Fig. 1), where the starting microstructure is austenite (β phase), is that strain recovers just by unloading when parasitic creep effects are avoided.

In many application of Cu-based SMA (e.g., CuAlBe), such as in civil engineering dampers, requires that the alloy does not increase its remnant strain when series of cycles are imposed. Any progressive 'creep' or permanent deformation (plastic and/or stabilization) in expected (guaranteed) amplitudes need to be avoided. A progressive increase of permanent deformation decreases the efficiency of the damper for solicitations with low amplitudes. Built dampers in civil engineering applications require relative cheap devices. For instance, use of polycrystalline Cu-based alloys as the CuAlBe.

In this work (paper II of this series) concern in Cu–Al–Be alloy in pseudoelastic (or superelastic) state, we analyze the effect of thermal treatments in grain growth to obtain a low accumulative creep in tensile stress cycling. The standard heat treatment for Cu-based alloys, in order to avoid inhomogeneities and stabilized martensite, consists in an appropriate homogenization or betatization treatment (short or long time at high temperature, i.e. 1123 K) followed by water quenching at room temperature and further aging. The temperature of 1123 K represents a compromise between sufficient mechanical strength of the alloy at this temperature and complete betatization, i.e., eliminate unwanted precipitates, stabilized martensite and inhomogeneities in the wires and/or bars. An important effect of the thermal treatments is to produce a considerable grain growth. The main target of this work relates to the evaluation of a phenomenological rule between time allowed at 1123 K and the minimizing of the permanent accumulative strain due to stress cycling. The dynamics of the grain growth related to the thermal treatment is also experimentally observed for some wire and bar diameters. The grain growth process shows an increased complexity when the grain diameter approaches the sample diameter.

The paper I of this series center in the action of thermodynamic forces acting on SMA in Cu-based alloys [14] and the series of papers in preparation are devoted to criteria for parameters estimation (i.e., Clausius–Clapeyron coefficient in CuAlBe and in NiTi) diffusion actions in NiTi and, in general, long time applications of SMA as in civil engineering or in mechanical engineering, the appropriate and representative models and, eventually, the simulation.

Experimental

The behavior of CuAlBe alloy is analyzed using wires and bars of different diameters furnished by Trefimetaux (Centre de Recherche, Serifontaine, France) and produced from similar casts. Table 1 shows the nominal chemical composition and the transformation temperatures of those casts. The extruded bars (3.4 and 15.1 mm diameter) are produced from AH140 cast. Thinned wires, after additional drawing, came from AH38 cast. For instance, the nominal squared cross section 1.2×1.2 mm^2 and other thinner diameters are prepared from cast AH38. The table shows the typical scatter in transformation temperatures, close to ±3 K, for 'equal' composition materials.

From the 'as furnished' material, samples were introduced in the furnace at 1123 K for different time

Table 1 Nominal data for the used wires of CuAlBe alloy. Composition in mass% and associated transformation temperatures for the two casts used

Cast	Nominal composition/mass%	Transformation temperatures/K
AH38	Al 11.8; Be 0.5; Cu 87.7	Ms=251; Mf=234; As=258; Af=271
AH140	Al 11.8; Be 0.5; Cu 87.7	Ms=255; Mf=226; As=253; Af=275

Ms, Mf – martensite start and finish, As, Af – austenite start and finish

intervals and then quenched in water. The samples are studied at two levels. The first one visualizes the grain growth. The second one ('usefulness of the samples for damping') is centered in the appropriate aging of the samples i.e., two steps at 373 and 323 K, and their 'creep response' to series of cycles (suitable mechanical testing). In other words, the practical behavior (the permanent accumulative strain) is evaluated with the grain diameter.

The grain size was determined after mechanical and chemical polishing. Grain size was determined through area quantitative metallography performed using optical microscopy. Thus, the mean squared grain radius, $\langle r^2 \rangle$, was calculated from measurements of the total area observed, A, and of the total number of grains in that area, N, employing $\langle r^2 \rangle = A/(N\pi)$.

The grain growth

Grain growth was studied for several wires of the CuAlBe alloy. In Fig. 2 the A–B–C–D frames shows the progressive grain growth for a squared cross section wire of 1.2×1.2 mm^2 associated to the time inside the furnace at 1123 K. The figure suggests the appearance of a chained grain structure for furnace times near 2 min. The general properties of chained grains are, usually of a deep theoretical interest [20]. Figure 3 shows the change of surface grain for a wire of 3.4 mm of diameter after 40 min at 1123 K, compared with the 'as furnished' wire. The observed samples did not present extreme grain aspect ratios which could have induced complexities in the measurements [21].

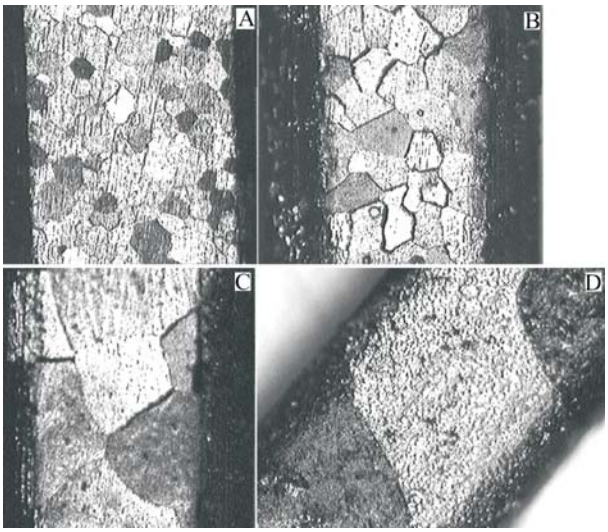

Fig. 2 Grain growth at 1123 K on a longitudinal observation of a 1.2×0.2 mm^2 section wire of the CuAlBe alloy, after a heat treatment at 1123 K, for different holding times: A – initial state, B – 9 s, C – 50 s and D – 150 s. The width of each metallographic sample, as seen on the photographs, is 1.2 mm

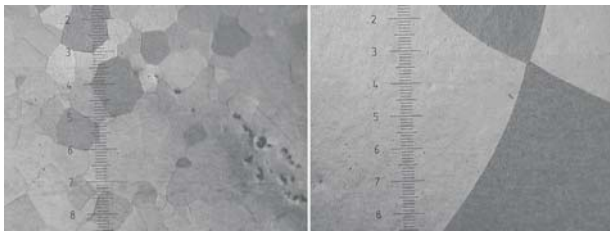

Fig. 3 Grain growth at 1123 K observed on a cross section of a 3.4 mm diameter (wire of CuAlBe); left – as-received microstructure; right – after 40 min. The vertical scale represents 0.7 mm

Transient sample-temperature evolution

The sample temperature evolution after introduction in a furnace at 1123 K is close to a transitory behavior modified by particular characteristic of the sample. Figure 4 shows temperature *vs*. time curves for a wire of 3.4 and a bar of 15.1 mm diameter (determined by a K-thermocouple). This evolution can be approximately described by an exponential approach, the time constant (τ) being a function of sample diameter (d): respectively 29 and 156 s for 3.4 and 15.1 mm diameter. From the above experimental data a rough heat-transfer model of temperature evolution can be proposed, having in mind a basic relationship between τ and d. For a long cylinder (heat capacity C and surface coupling P) surrounded by an external constant temperature, the time constant reads

$$\tau \approx C/P \propto d^2/d \propto \mathrm{d} \qquad (1)$$

For the two samples considered in Fig. 4, the time constant ratio is 0.19 and the diameter ratio is 0.23, ratio values which are in reasonable agreement between them. In other words, that the crude model (proportionality between τ and d) is satisfactory.

In the curves of Fig. 4, a perturbation 'a' can be observed near 870 K. Such perturbation can be ascribed to a dynamic phenomena related with phase transformation (i.e., precipitation and re-dissolution in the austenitic matrix). On the other hand, these curves show that for these heat treatments, a minimal time to attain furnace temperature is required: about 150 or 600 s for samples of 3.4 or 15.1 mm diameter, respectively. Extrapolation of these data to the wire of 1.2×0.2 mm^2 section indicates that the correct betatization of this wire has to be considered problematic for the B and C micrographs in Fig. 2: the wire temperature seems that remains under 800 K.

Grain growth and activation energy (wire diameter: 3.4 mm)

Figure 5 shows the experimental mean squared grain radius *vs*. the time inside the furnace at 1123 K. The $\langle r^2 \rangle$ values are estimated from the mean of two (or

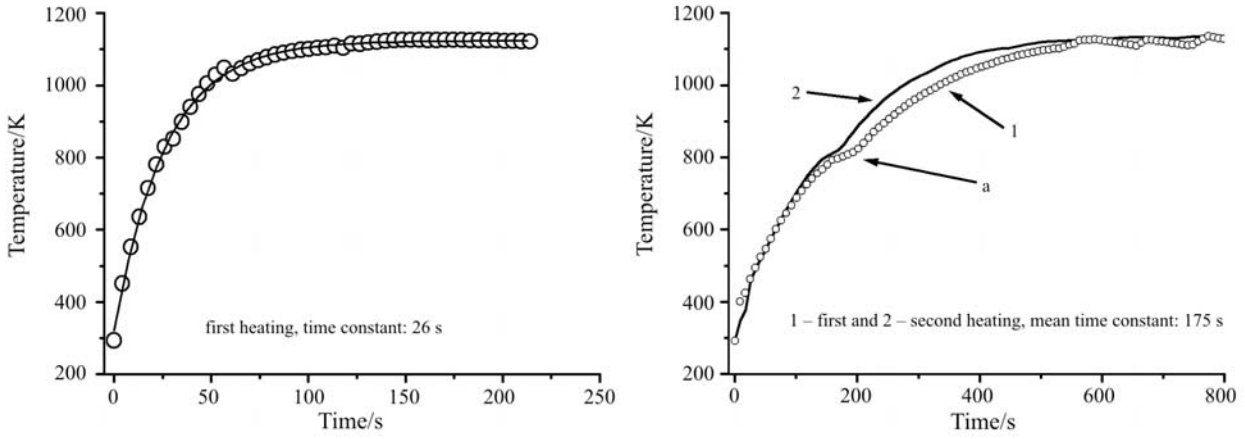

Fig. 4 Temperature evolution on heating for a CuAlBe alloy wire; left – sample of 3.4 mm of diameter. ○ – experimental, continuous line – exponential fit; right – sample of 15.1 mm of diameter. Time equal 0 is the introduction in the hot furnace at 1123 K; a – see text

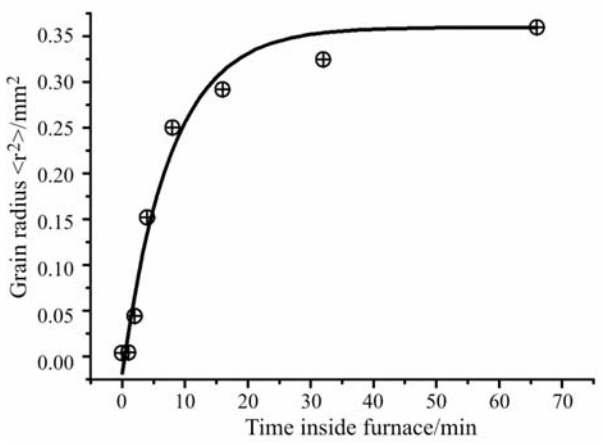

Fig. 5 Grain growth for CuAlBe wire of 3.4 mm diameter. Average of squared radius (<r^2>) *vs*. time inside the furnace at 1123 K. Dots – experimental data, continuous line – exponential fit (mean time constant 7.8 min)

three) sample sections. A rough approach to <r^2> is determined by the sample cross section divided by the product $N\pi$ where N is the number of observed grains. An elementary exponential fit between <r^2> and time furnishes a time constant close to 7.8 min. The grain growth proceeds quite fast. Non-homogeneities or parasitic gradients in the internal furnace temperature are to be avoided, or grains might grow irregularly, much larger in one part of the sample than in other parts, producing asymmetries inducing – at the application level – supplementary internal stresses and fragility.

The first part of the growth is practically linear between the observed mean squared radius (or squared diameter) and the time according to the expected classical approach i.e., normal and stable grain growth [20]. In fact, the observations indicate that, for this wire and furnace temperature, the grain growth proceeds very slow after 40 min at 1123 K. By using the grain diameter, for the first part of grain growth data, up to 10 min, the relation (2) is satisfied:

$$D^2 - D_0^2 = Kt \qquad (2)$$

After some 10 min the curvature suggests a change of the grain growth mechanism, i.e., appearance of interactions with the external sample surface.

The effect of using other furnace temperatures was tentatively considered. Furnace temperatures too high could mean local melting of the samples and changes in shape, and too low temperatures are dangerous because of the precipitation–dissolution at near 800–900 K, so 1123 K is a good compromise (higher than precipitation, lower than excessively weak material). Some observations of grain growth were done at 1073 K, and the initial grain growth was compared with the grain growth at 1123 K. This allowed the extraction of a very rough estimation of the activation energy for the $K(T)$ in Eq. (1), as near $1.5 \cdot 10^5$ J mol^{-1}. This value is relatively close to the activation energy estimated in [22] for the grain growth in CuAlZn, and also not too far from the value for pure Cu, $1.2 \cdot 10^5$ J mol^{-1}.

Grain growth for wire diameter 15.1 mm

Grain growth was also evaluated for a bar of the CuAlBe alloy (diameter: 15.1 mm). Figure 6 shows the experimental data.

From $D^2=D^2(t)$ a linear representation furnishes a regression coefficient greater than 0.99 and according with

$$D^2 - D_0^2 = Kt \rightarrow D^2 - D_0^2 = K(t - t_0)$$
$$\text{when } t_0 \rightarrow t \Rightarrow \mathrm{d}(D^2)/\mathrm{d}t = K$$

Thus, the slope in the Fig. 6 left is, directly, the K value. In this rough approach: $7.9 \cdot 10^{-4}$ mm^2 s^{-1}. In general, a representative model of grain growth reads,

$$D^n - D_0^n = Kt \qquad (2')$$

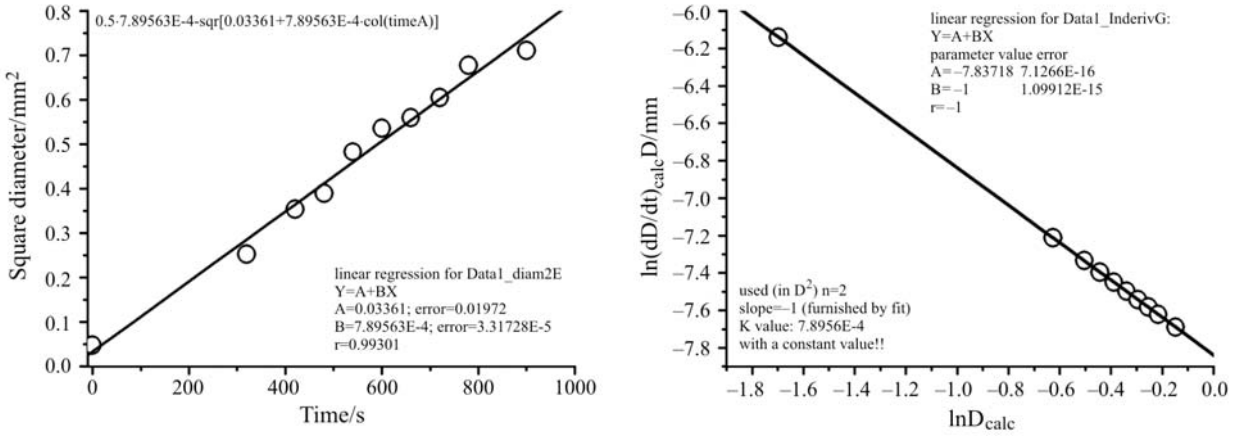

Fig. 6 Left – grain growth *vs*. time for a rod of 15.1 mm diameter; right – constancy of the mechanism of grain growth (see the text)

or, in local conditions

$$d(D^n)/dt=K \qquad (2")$$

where n is an exponent related to the mechanism, D_0 is the initial diameter, D the diameter after the time t and K it is a value that depends on the temperature and the mechanism, according to an activated process (energy E for each mechanism) as,

$$K=K_0\exp(-E/RT) \qquad (3)$$

Considering that the fit in Fig. 6 (left) can be analyzed as a series of successive short time-duration intervals (or temperature steps), it is possible to numerically determine the values of n and K. Note that for each interval, K is constant because the temperature is constant, while the value n is constant because the grain growth mechanism is unique. Thus, deriving the Eq. (2') *vs*. time and applying logarithms, it reads,

$$\log(dD/dt)=\log(K/n)+(1-n)\log D \qquad (4)$$

Equation (4) is outlined in Fig. 6 right. In a general behavior, the graph allows us to obtain the value of n from the local slope of the curve (equal to $(1-n)$) and the local K value using Eq. (2'). From Fig. 6 right, established with the experimental available data, n is effectively constant and equal to 2. For the time interval investigated, the grain growth mechanism has not changed, indicating that the intervention of external surfaces is still irrelevant. The good linear behavior of Fig. 6 right is, probably, influenced by the smoothing of data scatter proper of a log–log plot.

Usefulness of the samples for damping

For guaranteed damping purposes it is needed that the samples do not accumulate easily plastic deformation. A fine grained, thick polycrystalline sample of shape memory alloy has in each cross section of the sample some grains with non-favorable crystallographic orientation to produce strain when tensile stresses are applied and, then plastic deformation appears too easily. A very thin sample (which could be considered as a chain of grains) supports only small forces. A compromise in the cross section of the samples and the mechanical properties is needed. For CuAlBe polycrystalline alloy, a wire of 3.4 mm diameter can support forces in excess of some 2 kN, and has still low fragility with reasonable thermal treatment and aging times.

The thermal treatment at 1123 K produces grain growth. After the grain growth and the quench process is always convenient some aging at 373 K. Some lengthy time permits that the sample arrives to well-determined transformation temperature after the residual non-homogeneities of atomic order produced by quench are reduced and/or completely suppressed. Also an aging at temperatures close to room temperature value approaches the Ms to their steady value smoothing parasitic evolutions with the summer–winter external temperature changes.

Figure 7 shows the effects of aging in CuAlBe samples after the quench on the transformation temperature Ms. The sample was kept at controlled tempera-

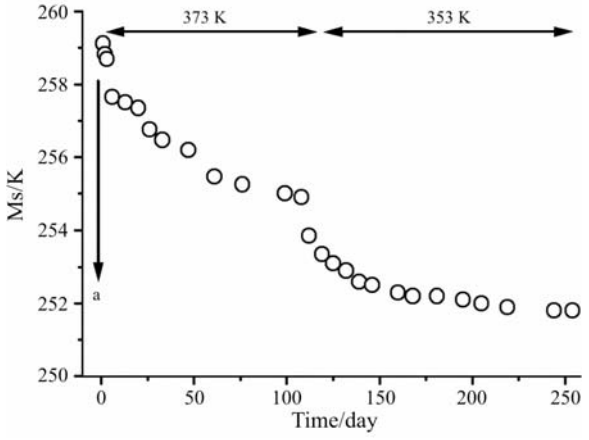

Fig. 7 Ms *vs*. aging time, at temperatures 373 and 353 K. The arrow a shows the initial quench processes

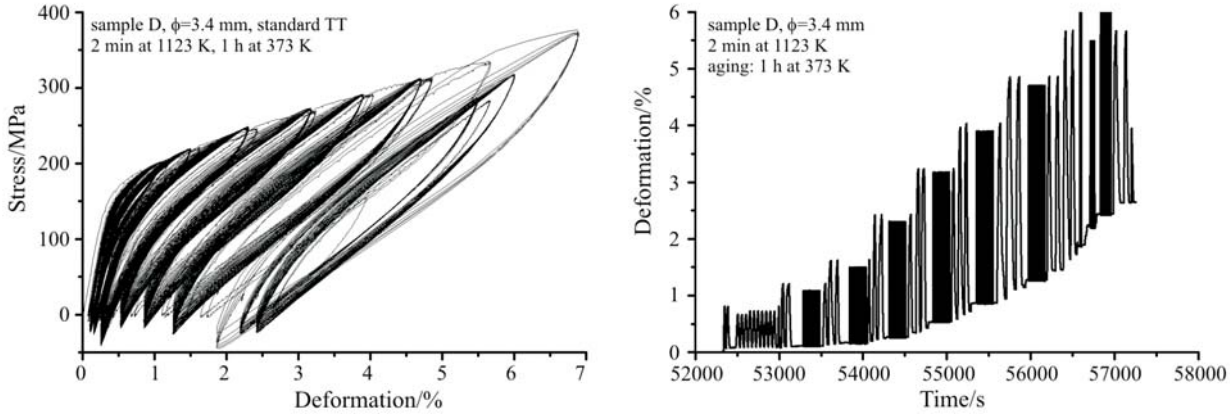

Fig. 8 The effect of increased deformation cycles in CuAlBe alloys; left – stress *vs*. strain, right – deformation *vs*. time for sets of cycles

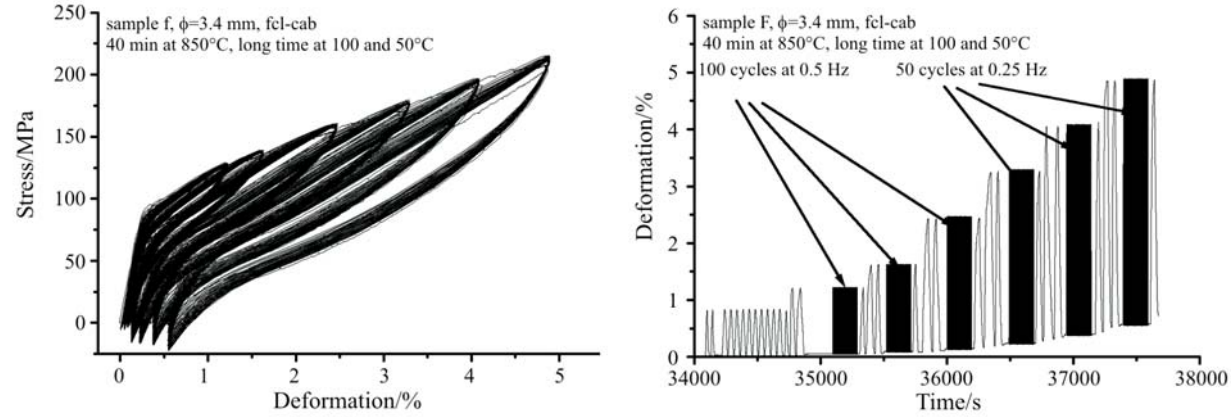

Fig. 9 The effect of increased deformation cycles in CuAlBe alloys for increased grain dimension and sample aging; left – stress *vs*. strain; right – deformation *vs.* time for a similar set of cycles as shown in the Fig. 8

ture, and from time to time, a programmed temperature cycle was performed, while measuring the electrical resistance, from which Ms values were determined. As can be seen from Fig. 7, a long aging at 373 K produces a decrease of near 5 K in Ms. Further aging at intermediate temperature (353 K) produces a supplementary Ms decrease (i.e., 3 K or more).

The expected effect of the grain growth is to determine a practical level without accumulative permanent deformation with cycling. In the damping application of SMA for scarce events as quakes the eventual accumulation of permanent deformation in cycling need to be avoided or carefully controlled [23–26].

Figure 8 left shows (in stress-strain coordinates) the effect of progressive amplitude of sets of cycles for a sample with a 'standard' heat treatment and, also, aging. Figure 8 right visualizes the progressive accumulation of deformation on cycling. For 3% of strain the permanent deformation overcomes 0.5% and the fracture stress overcomes 350 MPa. Figure 9 shows similar experimental observations for a sample with 40 min at 1123 K and a long time aging at 373 K and, after, at 323 K. For a deformation close to 4% the permanent accumulative creep do no overcomes 0.5% and the fracture level is situated near 250 MPa.

Conclusions

The experimental analysis suggests that an appropriate thermal treatment in polycrystalline samples permits the use of CuAlBe shape memory alloy for damping purposes with a reduced remnant deformation on cycling i.e., under 0.5% for pseudoelastic deformations close to 3.5%. The grains grow quite fast at the usual thermal treatment temperatures (1123 K). The increased grain diameter also reduces in some 30% the fracture stress level (from 350 to 250 MPa).

The observations establish that the grain growth for the application domain of the alloy (using wires of 3.4 mm of diameter) induces some complex interaction between surface grains and external surface of the samples. In this domain the grain growth saturates progressively and the standard linearity between the

diameter and the square root of time progressively decreases. For different wire diameters the grain grow process is highly affected by the external surface changing the mechanism of grow; i.e., for thinner wire is relatively easy to produce in a short time of betatization process a chain of grains with good mechanical behavior. For increased cross section, the interaction is more complex. An experimental roughly approach suggests the convenience of some particular evaluation for each type of wire.

Remark

The growth analysis can be studied only for relatively higher temperatures. At 'low temperatures' (i.e., near 800 or 900 K), the sample heating induces parasitic effects related with precipitation (i.e., of α phase) and subsequent re-dissolution ('a' in Fig. 4).

Acknowledgements

This research was supported by Spanish projects: MAT2002-10423E (MEC) and FPA2000-2635-E (M.F.), and by Chilean project Fondecyt 1030554. The cooperation between CIRG (UPC) and CAB-IB (University of Cuyo, Argentina) was supported by CNEA and, in the past, by DURSI (Gen. Catalonia). V.T. gratefully acknowledges the technical support from CAB-IB. In particular, experimental support from Mr. P. Riquelme and ideas in development of hand controlled devices from Mr. R. Stuke.

References

1 S. Saadat, J. Salichs, M. Noori, Z. Hou, H. Davoodi, I. Bar-on, Y. Suzuki and A. Masuda, Smart Mater. Struct., 11 (2002) 218.
2 G. Song, V. Chaudhury and C. Batur, Smart Mater. Struct., 12 (2003) 223.
3 M. Moallem, Smart Mater. Struct., 12 (2003) 1023.
4 N. Ma, G. Song and H.-J. Lee, Smart Mater. Struct., 13 (2004) 777.
5 Y. Luo, T. Okuyama, T. Takagi, T. Kamiyama, K. Nishi and T. Yambe, Smart Mater. Struct., 14 (2005) 29.
6 K. Otsuka and C. M. Wayman Ed., Shape Memory Materials, Cambrigde University Press, 1998.
7 R. Artiaga, A. Garcia, L. Garcia, A. Varela, J. L. Mier, S. Naya and M. Grana, J. Therm. Anal. Cal., 70 (2002) 199.
8 V. Brailovski, S. Prokoshkin, P. Terriault and F. Trochu Eds, Shape Memory Alloys: Fundamentals, Modeling and Applications, Université de Quebec, Ecole de Technologie Supérieure, ISBN 2-921145-42-1 (2003).
9 A. Varschavsky and E. Donoso, J. Therm. Anal. Cal., 63 (2000) 397.
10 A. Varschavsky and E. Donoso, J. Therm. Anal. Cal., 73 (2003) 167.
11 A. Isalgué and V. Torra, J. Thermal Anal., 52 (1998) 773.
12 F. C. Lovey and V. Torra, Progr. Mater. Sci., 44 (1999) 189.
13 V. Torra, A. Isalgue and F. C. Lovey, J. Therm. Anal. Cal., 66 (2001) 7.
14 V. Torra, J. L. Pelegrina, A. Isalgue and F. C. Lovey, J. Therm. Anal. Cal., 81 (2005) 131.
15 P. Nero, E. Mola, F. J. Molina and G. E. Magonnette, 'Full-scale PSD testing of a torsionally unbalanced three-storey non-seismic RC frame', 13th World Conference on Earthquake Engineering, Vancouver, B.C., Canada August 1–6, 2004, CD files, paper 968.
16 F. J. Molina, P. Buchet, G. E. Magonnette, O. Hubert and P. Nero, 'Bidirectional pseudodynamic technique for testing a three-storey reinforced concrete building', 13th World Conference on Earthquake Engineering, Vancouver, B.C., Canada August 1–6, 2004, CD files, paper 75.
17 M. O. Moroni, R. Saldivia, M. Sarrazin and A. Sepulveda, Mater. Sci. Eng., A335 (2002) 313.
18 V. Torra, A. Isalgue, F. Martorell, F. C. Lovey, M. Sade and F. J. Molina, 'From physical time dependent properties to guaranteed shape memory alloy dampers', 13th World Conference on Earthquake Engineering, Vancouver, CA, August 2004, CD files.
19 V. Torra, A. Isalgue, F. C. Lovey, F. Martorell, J. Molina and H. Tachoire, J. de Physique IV France, 113 (2004) 85.
20 W. W. Mullins and J. Viñals, Acta Materialia, 50 (2002) 2945.
21 S. D. Wher and J. M. Shaw, Can. Metall. Q., 41 (2002) 365.
22 J. Gil, J. M. Guilemany and J. Fernandez, Mater. Sci. Eng., A241 (1998) 114.
23 V. Torra, A. Isalgue, F. C. Lovey and M. Sade, 'Damping via Cu–Zn–Al shape memory alloys (SMA): the action of diffusive effects on the macroscopic description', S.-C. Liu, D. J. Pines, Eds, in Smart Structures and Materials 2002: Smart Systems for Bridges, Structures and Highways, Proceedings of SPIE, Vol. 4696 (2002), pp. 186–196.
24 V. Torra, A. Isalgue, F. C. Lovey and M. Sade, 'Thermomechanical properties of SMA', Proc. of 3rd World Conference on Structural Control, Vol. 2, Como (Italy) 2002, pp. 151–156.
25 F. C. Lovey, M. Sade, V. Torra, A. M. Condo and A. Isalgue, 'Some important properties of SMA regarding to civil engineering applications', Proc. of 3rd World Conference on Structural Control, Vol. 2, Como (Italy) 2002, pp. 157–162.
26 A. Isalgue, V. Torra and F. C. Lovey, 'Cu-based SMA: Quantifying and guaranteeing the time and temperature dependence on damping', Proc. of 3rd World Conference on Structural Control, Vol. 2, Como (Italy) 2002, pp. 363–368.

Received: December 1, 2005
Accepted: February 3, 2006
OnlineFirst: May 23, 2006

DOI: 10.1007/s10973-005-7480-3